STUDY OF AERODYNAMIC PERFORMANCE OF REAR TRUNK LIP SPOILER ON A PASSENGER CAR

Abubakar Isah[1*], Muhammad Uba Abdulazeez[2], Mansur Aliyu[3], Ibrahim Yahuza[4]

[1,4]Automotive Engineering Department, Air Force Institute of Technology, Kaduna-Nigeria
[2,3]Department of Automotive Engineering, Abubakar Tafawa Balewa University Bauchi-Nigeria
[2]Department of Mechanical Engineering, United Arab Emirates University
Corresponding Author: dankade@hotmail.com

Received: March 20, 2022 **Accepted:** June 18, 2022

Abstract: Today different types of spoilers are used on cars that are not heavy at the rear to serve as aerodynamic aids to improve their performance. The trunk spoiler functions as a barrier to the airflow passing, so that more pressure is built up above the rear trunk surface. This pressure resulted in inducing a force acting vertically downwards to decrease the car lift force. For this reason, this study is focused on the investigation of aerodynamic performance of lip spoiler on rear trunk of a passenger car. All of the analyses and modifications in this study were carried out using the computational fluid dynamics (CFD) software "ANSYS Fluent 15.0" and the CAD modelling in "AutoCAD 2015". The results of the simulation showed that adding the lip spoiler on the trunk resulted in a significant decrease in lift coefficient of the car by 95.0%. However, the drag coefficient of the car was increased by 2.25%. The results of the study were found to be in agreement with the effect of spoiler reported in the literature. Therefore, adding a lip spoiler on the rear trunk of a passenger car will improve the stability and performance of the car.

Keywords: Drag coefficient, Fuel efficiency, Lift coefficient, Performance, Stability, Turbulence

Introduction

During the motion of a car through the air, aerodynamic forces (lift and drag) and moments are acted upon. These forces arise due to the air flowing over the car and around it thereby affecting its performance and fuel economy. As reported in (Srinivas, 2016), (Kamacı & Kaya, 2021) and (Schuetz, 2016) about 50-60% of the entire fuel energy of cars is gone only to overcome the drag force which is resisting the forward motion of the car. Therefore, decreasing aerodynamic drag adds considerably to improving the fuel economy and reducing the CO_2 emissions of a car. Studies have found that the rear geometry of a car alone contributes about 40% of the total drag (Vinayagam et al., 2017). Again, cars generally become light at the rear end when cruising at high speed due to the effect of low pressure created on the trunk surface (Ragavan *et al*., 2014). The significant effect of this low pressure produced in measuring the performance of a car is noteworthy because it reduces its tire ground adhesion and hence, it reduces its stability and performance (Ahmed & Chacko, 2012). The consequences of increasing the car weight at the rear for instance to increase its tire ground adhesion for better performance cannot be exaggerated (Ahmed & Chacko, 2012; Srinivas, 2016; Verma *et al*., 2021). However, as far as the performance of a car is concerned, the induction of downforce to increase its tire ground adhesion is a prime factor. To abate the problems, redesigning the car body by making it more streamlined has been pronounced as an approach for decades (Kumar et al., 2019). As such, today, many aerodynamic aids can be noticed used in the automotive industries to mitigate the influence of regions in the car that immensely affects its performance (Ahmed & Chacko, 2012). Such aids, for instance, include flaps, deflectors, spoilers (upturned wing or lip-type), and vortex generators among others.

Spoilers attached to rear trunk of car is one of the efficient, most extensive and important aerodynamic aids used to improve car performance, see Figure. 1. Figure. 1a and Fig. 1b respectively show the lip-type and the inverted wing-type rear trunk spoilers used on cars. They both functions as a barrier to airflow so that high pressure is built up above the trunk surface area of the car (Mokhtar & Durrer, 2016; Nath et al., 2021). Srinivas (2016) described the lip-type spoiler as an excellent choice for a motorist who prefers a subtler and similarly appealing upgrade. This high pressure pushes the car down, thereby decreasing the car lift force and thus, increasing its tire ground adhesion without increasing the car weight at the rear. With this gain, the rear trunk spoiler, however, induces drag force that adds to the car total drag while some spoilers added have either little or no aerodynamic benefits *(Nath et al., 2021; Rossitto et al., 2017; C. S. Yuan et al.*, 2017). As reported, studies have established that when a spoiler is optimized with the car shape it can reduce the induced drag at a higher speed (Dominy, 2002; Ravelli & Savini, 2018; Seralathan *et al*., 2019; Verma et al., 2021; Z. Yuan & Wang, 2017).

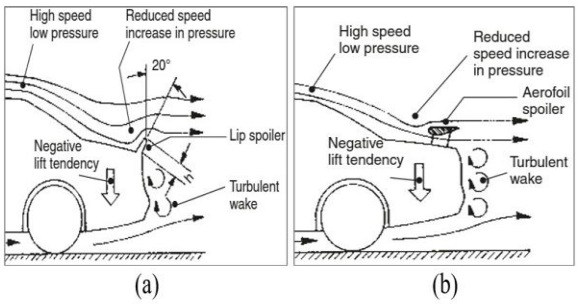

Fig. 1. Trunk spoilers

A lot of scientific studies have been carried out to improve aerodynamic performance of cars to conclude the effectiveness of spoilers using computational fluid dynamics (CFD) and experimental methods. The numerical method of CFD is extensively employed for aerodynamic analysis to optimize initial design calculations at a lesser expense. Additionally, CFD considerably offers additional data, such as the effect of three-dimensional vortices, which cannot be easily obtained experimentally (Lawal et al., 2015; Merryisha & Rajendran, 2019). In addition to the high cost of wind tunnel testing, they may also suffer from scaling effects. As a result, the CFD method has become a veritable design tool significantly employed in car aerodynamic study, mostly in speeding up the design and development of modern cars. For example, at a steady-state, Saifur-Rahman and Yadav (2018) studied the effect of rear wing-type spoiler and diffuser angles on aerodynamic characteristics of a sedan car at various speeds using standard k-ε turbulence model. They found that with an increase in the angle of inclination of the spoiler, the drag coefficient increases as well as the negative lift. From the

results also, the maximum and minimum values of the coefficient of drag (Cd) was at 2° and 5° inclination angles of the spoiler at 70 kmph and 140 kmph respectively. On the other hand, the maximum and minimum values of coefficient of lift (Cl) was at 2° and 13° inclination angles of the spoiler at 70 kmph and 90 kmph respectively. Again, Seralathan et al. (2019) carried out an aerodynamic-enhancement of Formula SAE car using split rear wings using STAR CCM+. The flow is considered as turbulent and the k-□ turbulence model was selected for the study. The outcomes found from the numerical study revealed that split rear wings reduced the car drag by 12% and increased the downforce by 38%. The author furthered that with the outcomes of the study, the car cornering speed and overall fuel efficiency is improved.

Another different study in (Kumar et al., 2015) examined drag and lift forces over the profile of a car with a rear wing-type spoiler using CFD. The study revealed that at all the speed cases considered, the wing-type spoiler attached to the trunk increases the amount of negative lift force generated while increasing the drag coefficient. Verma et al. (2021) determined the effect of the height of a lip-type spoiler of a small passenger car on aerodynamic performance. The study revealed a reduction in the drag force with the rise in the spoiler angle, while lift force was found reduced at a smaller spoiler angle. However, more rise in the lift force was spotted with the rise in spoiler angle. Again, the study further revealed the lift force at the higher spoiler angle was lower than the lift produced by the baseline car. Also, 60-100° of the lip spoiler angle was found to be the optimal angle to reduce both drag and lift.

Similarly, Nath et al. (2021) studied drag reduction by application of aerodynamic devices in a race car using standard k-ε turbulence model. The simulation results show that by only adding a lip-type spoiler at the rear edge of the trunk lid, both the drag and lift forces reduces considerably. This is inconsistent with the findings in (Verma et al., 2021) and (Seralathan et al., 2019) as regards the drag force. Again, Hortelano-Capetillo et al. (2020) in a similar way investigated the lift and drag forces for sedan cars with six (6) different lip spoiler heights using the standard k-ε turbulence model. In the study, the overall aerodynamic performance of the car with the lip spoiler was improved. The study revealed the lift force to be decreased significantly as the height of the spoiler increases although the drag force was almost constant for all the designs. The study further revealed that the spoiler with 0.1 m base and 0.08 m height offers a better tradeoff by reducing the lift force to 44.5% while drag increased up to 3.5%.

On the whole, all the studies presented demonstrated that attaching a spoiler either the inverted wing-type or the lip-type on a car rear trunk affects its aerodynamic performance. Again, it was seen that a compromise is required for optimum effectiveness. For this reason, this research is focused on the investigation of a rear trunk lip-type spoiler effect on the aerodynamic performance of a passenger car. The car is generic and it is modelled in AutoCAD 2015 software. The analysis method employed is CFD which is inexpensive and has the advantage of repeatability using the standard k-ε turbulence model with enhanced wall function. The rest of this paper is structured as follows: Section 2 describes the methodology. Section 3 provides the simulation results and discussion. Section 4 concludes the paper.

Methodology

In this study, the generic passenger car model was designed in AutoCAD 2015 software as well as all the needed modifications. The model was imported into ANSYS Fluent design modeller 15.0 software for the study. The investigation involves simulation in a virtual wind tunnel, a computational domain (CD) that is designed in the ANSYS Fluent interface. Table 1 shows the basic measurements of the generic car model. Figure. 2 presents the baseline passenger car model produced, while Figure. 3 shows the model fitted with the lip-type spoiler on the rear end of the trunk in an attempt to minimize the overall lift and drag coefficients. Figure. 4 shows the passenger car model in the computational domain designed for the simulation.

Table 1. Basic measurements of the generic passenger car model

Section	Dimensions
Wheelbase	3400 mm
Height	1300 mm
Front overhang	900 mm
Rear overhang	1500 mm
Wheel (r)	330.25 mm
Width	2100 mm
Lip spoiler height	100 mm
Lip spoiler base	80 mm
Lip spoiler angle	63.5°

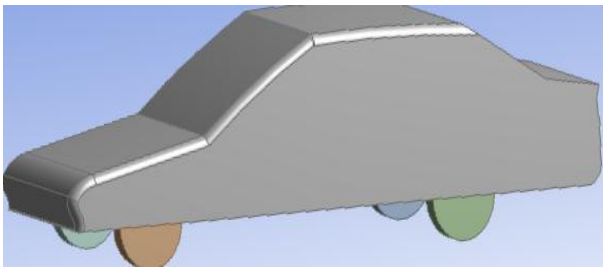

Fig. 2: Baseline model

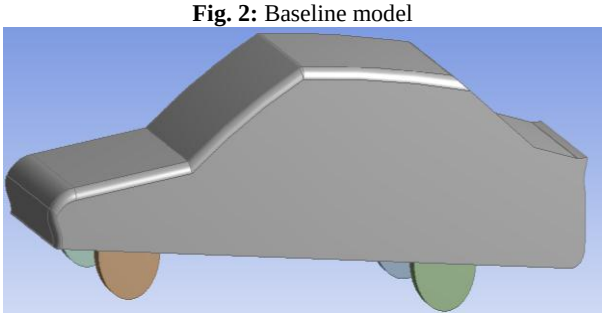

Figure 3. A modified model with trunk lip spoiler

Steps of the Analysis

Boundary specifications

The specifications of the boundary are done after the import of the car model and the computational domain has been designed. The face of the computational domain (CD), 'inlet' was selected and named "Velocity Inlet" and the face opposite to it was selected and named as "Pressure Outlet", (see Figure 4.). The model under investigation was named "Car". The Symmetry planes are named "Symmetry", the bottom and the top surfaces were named "Road" and "Wall" respectively.

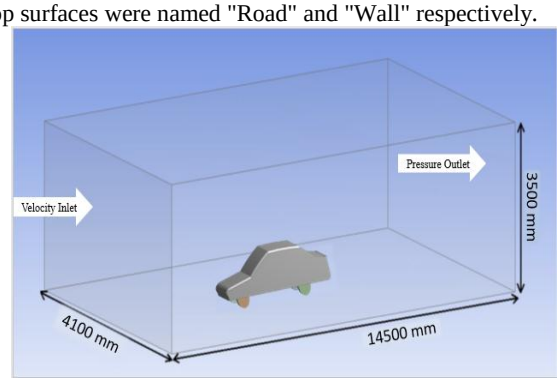

Fig. 4. Passenger car model in the computational domain

Meshing option

The meshing options used in this investigation are shown in Table 2. The surface unstructured mesh was performed on the models as well as on the surface of the computational domain. Figures 5 and 6 present the mesh produced in the baseline model and model with the trunk lip spoiler together with computational domain respectively.

Table 2. Meshing options

Object name	Option
State	Solved
Physics preference	CFD
Solver preference	Fluent
Relevance centre	Fine
Smoothing	High
Span angle centre	Fine

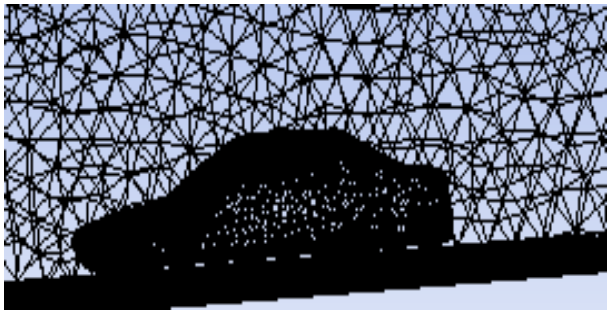

Fig. 5: Surface mesh performed on the baseline model

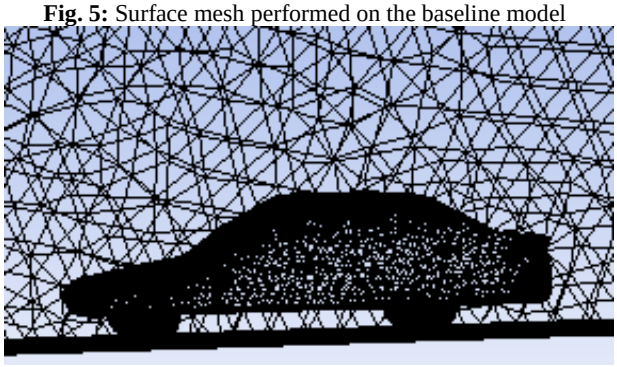

Fig. 6: Surface mesh performed on a modified model with a trunk lip spoiler

Simulation setup

"Double Precision" was carefully chosen to perform the simulation. A pressure-based solver was considered which is primarily for low-speed incompressible flow. The standard k-ε turbulence model was selected to be used as one of the most commonly used Reynolds Average Navier-Stokes (RANS) turbulence models that suit the workhorse of practical engineering flow calculations (Levin & Rigdal, 2011). The ANSYS Fluent CFD solver uses the Navier-Stokes equations which are composed of continuity and momentum on average. The total velocity, u_i is decomposed as a function of the mean velocity $\overline{u_i}$ and the fluctuating component $\acute{u_i}$ as shown in Equation. (1). In the same manner, the average can be applied to all other flow variables as shown in Eq. (2) for the pressure variable.

$$u_i = \overline{u_i} + \acute{u_i} \quad (1)$$

$$p = \bar{p} + \acute{p} \quad (2)$$

The continuity and momentum equations incorporating the instantaneous flow variables are given in Eq. (3) as:

$$\frac{\partial}{\partial x_i}(\overline{u_i}) = 0 \quad (3)$$

$$\frac{D\overline{u_i}}{Dt} = -\frac{1}{\rho}\frac{\partial P}{\partial x_i} + \frac{\partial}{\partial x_j}\left[\mu\left(\frac{\partial \overline{u_i}}{\partial x_j} + \frac{\partial \overline{u_i}}{\partial x_i} - \frac{2}{3}\delta_{ij}\frac{\partial \overline{u_k}}{\partial x_k}\right)\right] + \frac{\partial}{\partial x_j}\left(-\overline{\acute{u_i}\acute{u_j}}\right) \quad (4)$$

The above equations are known as the RANS equations where u, ρ and μ represents the velocity, density and dynamic viscosity of the fluid. The term $-\overline{\acute{u_i}\acute{u_j}}$ in Eq. (4) is known as the Reynolds stress tensor (RST) and is defined in Eq. (5). The RST accounts for the turbulent fluctuations and is required to be modelled to close the RANS equation. The modeling of the RST to obtain a solution requires some approximations in the governing differential equations at various levels of sophistication. The level of approximation employed in closing the RST leads to diverse turbulence models. One of such approximations employs the Boussinesq hypothesis, which relates the Reynolds stress and the mean velocity (Versteeg & Malalasekera, 2007), thus:

$$\left(-\overline{\acute{u_i}\acute{u_j}}\right) = \mu_t\left(\frac{\partial \overline{u_i}}{\partial x_j} + \frac{\partial \overline{u_j}}{\partial x_i}\right) \quad (5)$$

Different turbulence models have been seen used to predict different engineering problems, but each has its limitations (Roy et al., 2018). Today, numerous commercial and proprietary software have been developed for CFD analysis of various industrial and non-industrial flows. In this study, ANSYS-Fluent 14.0 CFD software is employed using the standard k-ε turbulence. As reported by Yakhot (1992) (as cited in (Hortelano-Capetillo et al., 2020)), the relation for the standard k-ε turbulence model is shown in Eq. (6) and (7).

$$\frac{\partial}{\partial t}(\rho k) + \frac{\partial}{\partial x_i}(\rho k u_i) = \frac{\partial}{\partial x_j}\left[\left(\mu + \frac{\mu_t}{\sigma_k}\right)\frac{\partial k}{\partial x_j}\right] + G_k + G_b + \rho\varepsilon + Y_M + S_k \quad (6)$$

$$\frac{\partial}{\partial t}(\rho \varepsilon) + \frac{\partial}{\partial x_i}(\rho \varepsilon u_i) = \frac{\partial}{\partial x_j}\left[\left(\mu + \frac{\mu_t}{\sigma_\varepsilon}\right)\frac{\partial \varepsilon}{\partial x_j}\right] + C_{1\varepsilon}\frac{\varepsilon}{k} + (G_k + C_{3\varepsilon}G_b) - C_{2\varepsilon}\rho\frac{\varepsilon^2}{k} + S_\varepsilon \quad (7)$$

In these Eq. (6) and Eq. (7), G_k and G_b represent the generation of turbulence kinetic energy due to the mean velocity gradients and buoyancy respectively. Y_M represents the contribution of the fluctuating dilatation in compressible turbulence to the overall dissipation rate. $C_{1\varepsilon}, C_{2\varepsilon},$ and $C_{3\varepsilon}$ are constant. σ_k and σ_ε are the turbulent Prandtl numbers for k and ε respectively. S_k and S_ε are user-defined source terms. The turbulent viscosity, μ_t is computed by combining the turbulent kinetic energy, k and the rate of dissipation of the turbulent kinetic energy, ε in Equation. (8) as follows:

$$\mu_t = \rho C_\mu \frac{k^2}{\varepsilon} \quad (8)$$

where C_μ is a constant.

The model constant $C_{1\varepsilon}, C_{2\varepsilon}, C_\mu, \sigma_k$ and σ_ε have the following widely accepted values determined from experiments. Depending on the situation, these values can be changed.

$C_{1\varepsilon} = 1.44, C_{2\varepsilon} = 1.92, C_\mu = 0.09, \sigma_k = 1.0,$ and $\sigma_\varepsilon = 1.3$

The production of turbulence kinetic energy, $G_k = \frac{\partial u_j}{\partial x_i}\left(-\rho\overline{\acute{u_i}\acute{u_j}}\right)$

To evaluate G_k in a manner consistent with the Boussinesq hypothesis,

$$G_k = \mu_t S^2$$

where S is the modulus of the mean rate-of-strain tensor, defined as

$$S \equiv \sqrt{2S_{ij}S_{ij}}$$

It is noteworthy that the Standard $k-\varepsilon$ turbulence model assumes that the flow is fully turbulent, and the effects of molecular viscosity are negligible. Thus, the model is valid for fully turbulent flows. The relationship between drag and lift forces is given in Eq. (9) and Eq. (10) respectively as obtained in (Vishal et al., 2018) and (Bayındırlı & Çelik, 2020). The lift force is the force that reduces the tire ground adhesion which is acting perpendicular to the car while the drag is the force acting relative to the direction of motion of the car to the surrounding air and is important in determining the performance of a car.

$$C_d = F_d/0.5\rho V^2 A \quad (9)$$

$$C_l = F_l/0.5\rho V^2 A \quad (10)$$

where F_d and F_l are the drag and lift forces correspondingly. C_d and C_l are the coefficients of drag and lift respectively, ρ is the density of the air, A is the frontal area of the car, and V is the relative speed. The drag and lift coefficients are valuable when equating the aerodynamic efficiency of different cars.

Boundary condition setting

The boundary employed in this research involved inlet velocity, which was taken to be 40 m/s as the velocity of the model at which it is moving and the surrounding air assumed incompressible. The pressure (gauge) at the outlet was taken into account to act in the direction perpendicular to the boundary.

Solution method and control

The lift and drag monitors were produced from the "Monitors'" section in which during the iterations their convergence values were determined. Table 3 presents the monitoring and convergence criteria set for this investigation

Table 3. Monitoring and convergence criteria

Equations	Flow and Turbulence
Monitor	Residuals, Lift and Drag coefficients
Convergence criteria	Continuity, epsilon, k, x, and y- direction = 0.0001 respectively

The Coupled scheme was considered which solves the momentum equation and pressure as coupled leading to quicker convergence, more sensible, and secure method (Gondipalle, 2011). Selections for "Spatial Discretization" are made sequentially in which the Gradient was chosen to be "Least Square Cell-Based," the "Pressure" to be 'Standard', the 'Momentum', 'Turbulent Kinetic Energy' and 'Turbulent Dissipation Rate' to be in 'Second Order Upwind' respectively.

Solution initialization and running the calculations

The setup was initialized using Hybrid initialization and the calculations were set to run for 400 iterations from the boundary conditions specified. Hybrid Initialization is a collection of recipes and boundary interpolation methods. It solves the Laplace equation to produce a velocity field that conforms to complex domain geometries, and a pressure field that smoothly connects high and low-pressure values in the CD. All other variables (that are temperature, turbulence, species, and so on) will be patched based on domain averaged values or a predetermined recipe (ANSYS Inc, 2013).

Results and Discussion

The CFD simulation is performed to study the aerodynamic performance of a baseline car model and a modified model with a trunk lip-type spoiler. Initially, the baseline model was tested and subsequently the modified model. To well understand the flow around the car, the pressure distribution contours and velocity vectors offer some insights. The results of the analysis conducted are shown in Figs. 7 – 10. Figs. 7 and 8 present the static pressure contour on the surface of the baseline model and the model with a lip spoiler respectively, while Fig. 9 and Fig. 10 show the velocity vectors on the surface of the baseline model and the model with a lip spoiler respectively. The pressure contours, Fig. 7 and Fig. 8, and the velocity vectors, Fig. 9 and Fig. 10 represent the magnitude pressure and velocity of the fluid and are used to identify the flow pattern and to study the regions liable for a high coefficient of drag and lift.

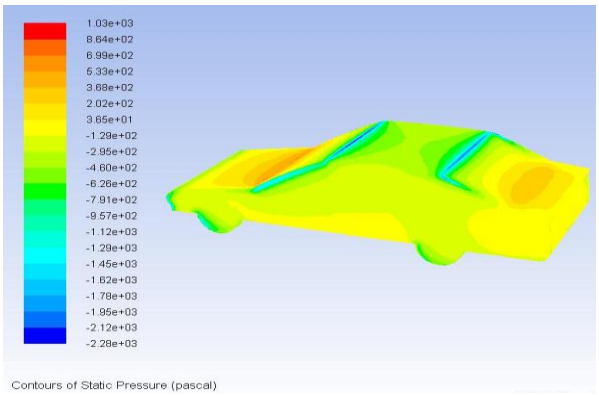

Fig. 7: Static pressure contour on the surface of the baseline model

From Fig. 7, the maximum static pressure at the trunk surface area of the baseline model was determined to be between 202 to 368 Pascal. This is reasonably below the pressure on the trunk surface area of a model with a lip spoiler shown in Figure 8, which is between 323 to 496 Pascal.

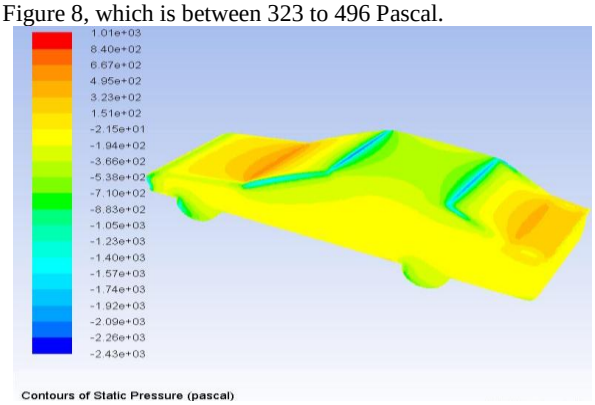

Fig. 8: Static pressure contour on the surface of the model with a lip spoiler

This proved that the spoiler has affected the aerodynamic performance of the car greatly. If so, this high static pressure seen on the trunk that has been developed confirmed that the model partakes in a greater negative lift force. Thus, a greater tyre ground holding. This finding is also in agreement with what was reported in (Ahmed & Chacko, 2012; Datta et al., 2019; Hortelano-Capetillo et al., 2020; Rossitto et al., 2017; Verma et al., 2021; Yuan et al., 2017) among others.

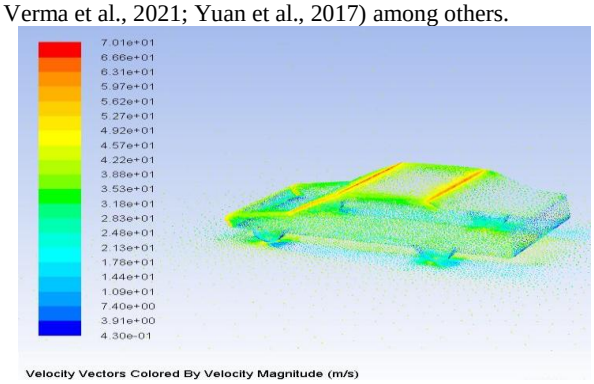

Fig. 9: Velocity vectors on the surface of the baseline model

Comparing Figs. 9 and 10, it is seen that more air has been trapped on the trunk in Fig. 10 than in Fig. 9. This trapped air results in an increase in negative downforce of the car by increasing the pressure on the trunk as seen in Fig. 10 thereby increasing the tyre ground adhesion. This action verifies the principle of Bernoulli. Moreover, this can be justified by relating the results obtained in Table 4 for the convergence of the coefficient of lift whereas the coefficient of drag increases as shown. This finding is also in agreement with what was reported in (Ahmed & Chacko, 2012; Datta et al., 2019;

Hortelano-Capetillo et al., 2020; Rossitto et al., 2017; Saifur-Rahman & Yadav, 2018; Yuan et al., 2017) among others. However, this is contrary to what was found in (Verma et al., 2021) and (Nath et al., 2021) as the drag was seen to be lessened.

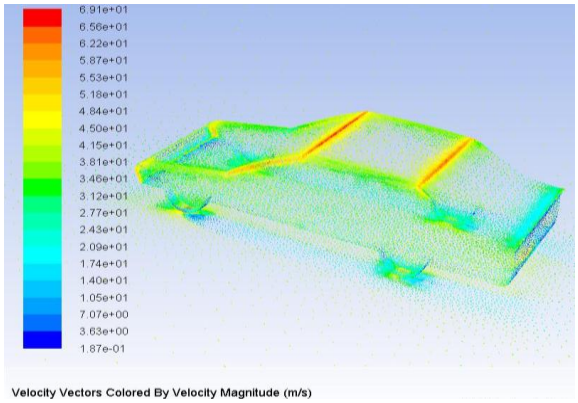

Fig. 10: Velocity vectors on the model with lip spoiler

Evaluating the flow around the car further, at the base of the car windshield there is significant pressure built up by the air molecules as at this point the air was stagnated. This was anticipated since for concave surfaces the velocity of the air slows down and the number of collisions of the air molecules increases. This is because the incoming air molecules will hit head-on and roughly may rebound back once more due to intermolecular collisions (Katz, 2016).

On the other hand, assessing the flow around the car once more at the leading and trailing edges of the car roof, the air molecules are seen to move at a very high speed and the pressure is moderately low. Similarly, the moderate-low pressure observed was anticipated as the flow is over a convex surface, both the leading and trailing edges of the car roof. At these regions of the car, the flow has been separated, the flow is thus turbulent. At the trailing edge of the car roof, the airflow separates forming a large wake. Schuetz (2016) furthered that the flow separates at the trailing edge of the car roof may or may not reattach on the trunk lid. This is where the impression for attaching a spoiler on a car trunk emerges to trap the air molecules to utilize it in creating negative lift or downforce to aid to push the car's tyre against the road and improve the cornering force. Flow separation is eventually a result of a strong adverse pressure gradient and is liable for a major part of the aerodynamic drag of a car. According to (Ahmed et al., 1987), for an increase in pressure in the flow direction, the boundary layer flow is retarded, particularly near the wall, and even reversed flow may occur. Furthermore, according to (Schuetz, 2016) flow reattachment will occur on a notchback, or in front of the windshield when it is fairly steep. It is worth mentioning that the car model investigated in this study is notchback.

Table 4 shows the relative results obtained for the drag and lift coefficients between the two model shapes. The results were extracted after the simulation had converged.

Table 4. Comparative results of the analysis

Shape	C_d	C_l
Baseline model	0.311	0.080
A modified model with a lip spoiler	0.318	0.004

As summarized in Table 4 the value for the coefficient of drag increased from 0.311 to 0.318 when the lip spoiler was attached, while the lift coefficient value decreased from 0.080 to 0.004 with the trunk lip spoiler. Thus, attaching the lip-type spoiler to the trunk affects the aerodynamic performance of the car and therefore, the car model with spoiler, Figure 3 will travel faster through a corner and will have better maneuverability, stability and performance. However, with an increase in fuel consumption due to the little increase in drag.

Conclusion

This research paper reports the aerodynamic performance of a lip spoiler on the rear trunk of a passenger car with a height, base and spoiler angle of 100 mm, 80 mm and 63.5º respectively. The outcomes of the analysis presented show that adding a spoiler affects the stability and aerodynamic performance of a car significantly. As cited, spoilers besides reducing the lift force, as mentioned, rarely decrease drag, which this study has demonstrated. The values obtained gave an idea about the behaviour of these models at a speed of 144 km/hrs. Similarly, the flow around the car was discussed.

References

Ahmed, H., & Chacko, S. (2012). Computational optimization of Vehicle Aerodynamics. *Annals of DAAAM for 2012 & Proceedings of the 23rd International DAAAM Symposium*, *23*(1), 313–318.

Ahmed, S. R., Emmelmann, H., Gengenbach, W., Hucho, W., Hummel, D., & Piatek, R. (1987). *Aerodynamics of Road Vehicles: From Fluid Mechanics to Vehicle Engineering* (W. Hucho (ed.); First). Butterworth-Heinemann Ltd.

ANSYS Inc. (2013). *ANSYS Fluent Theory Guide* (Vol. 15317, Issue November, pp. 724–746). SAS IP, Inc. U.S.A.

Bayındırlı, C., & Çelik, M. (2020). The determination of effect of windshield ınclination angle on drag coefficient of a bus model by CFD method. *International Journal of Automotive Engineering and Technologies*, *9*(3), 122–129.

Datta, B., Goel, V., Garg, S., & Singh, I. (2019). Study of Various Passive Drag Reduction Techniques on External Vehicle Aerodynamics Performance: CFD Based Approach. *International Research Journal of Engineering and Technology (IRJET)*, *06*(05), 1851–1871.

Dominy, R. (2002). An Introduction to Modern Vehicle Design. In J. Happian-Smith (Ed.), *Body design: Aerodynamics* (First, pp. 111–124). Butterworth-Heinemann.

Gondipalle, R. S. (2011). *CFD Analysis of the Under Hood of a Car for Packaging Considerations*. Clemson University.

Hortelano-Capetillo, G. J., Martínez-Vázquez, J. MercedZuñiga- Cerroblanco, J. L., & Rodriguez-Ortiz, G. (2020). Analysis of drag and lift forces for a sedan car using a rear lip spoiler. *Journal of Mechanical Engineering*, *4*(13), 23–31. https://doi.org/10.35429/JME.2020.13.4.23.31

Kamacı, C., & Kaya, K. (2021). Numerical Investigation of Aerodynamic Properties of Ahmed Body for Different Rear Slanted Surface Configurations. *European Journal of Science and Technology*, *28*, 469–475. https://doi.org/10.31590/ejosat.1005846

Katz, J. (2016). *Automotive Aerodynamics* (First). John Wiley & Sons, Ltd.

Kumar, R. B., Nitesh Varshan, M., & Kannan, T. (2019). Aerodynamic Design Optimization of an Automobile Car Using computational fluid dynamics approach. *Australian Journal of Mechanical Engineering*. https://doi.org/10.1080/14484846.2019.1654963

Kumar, V. N., Narayan, K. L., Rao, L. N. V. N., Ram, Y. S., & Kumar, V. N. (2015). Investigation of Drag and Lift Forces over the Profile of Car with Rearspoiler using CFD. *International Journal of Advances in Scientific Research*, *1*(08), 331–339. https://doi.org/10.7439/ijasr

Lawal, M. S., Thomas, S., Udeagulu, C., & Jemitola, P. O. (2015). Prediction of Aerodynamic Paramaters and

Pressure Distribition of the Wing of Gulma UAV. *3rd International Symposium on Engineering and Natural Science (ISEAN)*.

Levin, J., & Rigdal, R. (2011). *Aerodynamic analysis of drag reduction devices on the underbody for SAAB 9-3 by using CFD*. Chalmers University of Technology.

Merryisha, S., & Rajendran, P. (2019). Experimental and CFD Analysis of Surface Modifiers on Aircraft Wing : A Review. *CFD Letters*, *11*(10), 46–56.

Mokhtar, W., & Durrer, S. (2016). A CFD Analysis of a Race Car Front Wing in Ground Effect. *Proceedings of the 2016 ASEE North Central Section Conference*, 1–12.

Nath, D. S., Pujari, P. C., Jain, A., & Rastogi, V. (2021). Drag reduction by application of aerodynamic devices in a race car. *Advances in Aerodynamics*, *3*(4), 1–20. https://doi.org/10.1186/s42774-020-00054-7

Ragavan, T., Palanikumar, S., Anastraj, D., & Arulalagan, R. (2014). Aerodynamic Drag Reduction on Race Cars. *Journal of Basic and Applied Engineering Research*, *1*(4), 99–103. http://www.krishisanskriti.org/jbaer.html

Ravelli, U., & Savini, M. (2018). Aerodynamic Simulation of a 2017 F1 Car with Open-Source CFD Code. *Journal of Traffic and Transportation Engineering*, *6*, 155–163. https://doi.org/10.17265/2328-2142/2018.04.001

Rossitto, G., Sicot, C., Ferrand, V., Borée, J., Rossitto, G., Sicot, C., Ferrand, V., Borée, J., & Aero-, F. H. (2017). Aerodynamic Performances of Rounded Fastback Vehicle. *Proceedings of the Institution of Mechani- Cal Engineers, Part A: Journal of Power and Energy*, 1211–1221. https://doi.org/10.1177/0954407016681684%0AAny

Roy, A., Mallik, A. K., & Sarma, T. P. (2018). A Study of Model Separation Flow Behavior at High Angles of Attack Aerodynamics. *Journal of Applied Computational Mechanics*, *4*(4), 318–330. https://doi.org/http://dx.doi.org/10.22055/JACM.2018.24339.1183

Saifur-Rahman, M., & Yadav, K. (2018). Effect of Rear Spoiler and Diffuser Angle on Aerodynamic Characteristics of a Sedan. *International Journal of Research in Engineering*, *08*(June), 105–117.

Schuetz, T. (2016). *Aerodynamics of Road Vehicles* (Fifth). SAE International. https://doi.org/10.4271/r-430

Seralathan, S., K, B. B. S., I, G. V., Hariram, V., & T, M. P. (2019). Aerodynamic Enhancement Of Formula Sae Car Using Split Rear Wings. *International Journal of Scientific & Technology Research*, *8*(11), 694–699.

Srinivas, L. V. (2016). *Shape Optimization of a Car Body for Drag Reduction and to Increase Downforce* (Issue April) [Sree Vidyanikethan Engineering College, Tirupati]. https://www.researchgate.net/publication/301673979/download

Verma, R. P., Kumar Chaudhary, N., & Avikal, S. (2021). Effect of direction of lip spoiler on the aerodynamic performance of a small passenger vehicle. *Materials Today: Proceedings*. https://doi.org/https://doi.org/10.1016/j.matpr.2020.12.448

Versteeg, H. K., & Malalasekera, W. (2007). *An Introduction to Computational Fluid Dynamics* (Second). Pearson Education Limited.

Vinayagam, P., Rajadurai, M., Balakrishnan, K., & Priya, G. M. (2017). Design modification on Indian Road Vehicles to Reduce Aerodynamic Drag. *International Journal of Advanced Engineering, Management and Science (IJAEMS)*, *3*(8), 6–11. https://doi.org/10.24001/ijaems.3.8.6

Vishal, D., Tanuj, J., & Gurminder, S. (2018). Effect of Front Slant Angle on Aerodynamics of a Car. In A. Prasad, S. S. Gupta, & R. K. Tyagi (Eds.), *Advances in Engineering Design* (pp. 641–653). Springer Nature Singapore Pte Ltd. https://doi.org/10.1007/978-981-13-6469-3_59

Yuan, C. S., Mansor, S., & Abdullah, M. A. (2017). Effect of Spoiler Angle on the Aerodynamic Performance of Hatchback Model. *International Journal of Applied Engineering Research*, *12*(22), 12927–12933.

Yuan, Z., & Wang, Y. (2017). Effect of Underbody Structure on Aerodynamic Drag and Optimization. *Journal O of Measurements In Engineering. September*, *5*(3), 194–204. https://doi.org/10.21595/jme.2017.19210